Published online 10 November 2017 *Nucleic Acids Research, 2018, Vol. 46, No. 1* ***189–202***
doi: 10.1093/nar/gkx1010

Regulation of transcriptional silencing and chromodomain protein localization at centromeric heterochromatin by histone H3 tyrosine 41 phosphorylation in fission yeast

Bingbing Ren[1], Hwei Ling Tan[1], Thi Thuy Trang Nguyen[1], Ahmed Mahmoud Mohammed Sayed[2], Ying Li[3], Yu-Keung Mok[2], Henry Yang[3,4] and Ee Sin Chen[1,4,*]

[1]Department of Biochemistry, National University of Singapore, Yong Loo Lin School of Medicine, Singapore, [2]Department of Biological Sciences, National University of Singapore, [3]Cancer Science Institute, National University of Singapore, Yong Loo Lin School of Medicine, Singapore and [4]National University Health System (NUHS), Singapore

Received October 20, 2016; Revised October 07, 2017; Editorial Decision October 12, 2017; Accepted October 13, 2017

ABSTRACT

Heterochromatin silencing is critical for genomic integrity and cell survival. It is orchestrated by chromodomain (CD)-containing proteins that bind to methylated histone H3 lysine 9 (H3K9me), a hallmark of heterochromatin. Here, we show that phosphorylation of tyrosine 41 (H3Y41p)—a novel histone H3 modification—participates in the regulation of heterochromatin in fission yeast. We show that a loss-of-function mutant of H3Y41 can suppress heterochromatin de-silencing in the centromere and subtelomere repeat regions, suggesting a de-silencing role for H3Y41p on heterochromatin. Furthermore, we show both *in vitro* and *in vivo* that H3Y41p differentially regulates two CD-containing proteins without the change in the level of H3K9 methylation: it promotes the binding of Chp1 to histone H3 and the exclusion of Swi6. H3Y41p is preferentially enriched on centromeric heterochromatin during M- to early S phase, which coincides with the localization switch of Swi6/Chp1. The loss-of-function H3Y41 mutant could suppress the hypersensitivity of the RNAi mutants towards hydroxyurea (HU), which arrests replication in S phase. Overall, we describe H3Y41p as a novel histone modification that differentially regulates heterochromatin silencing in fission yeast via the binding of CD-containing proteins.

INTRODUCTION

Genomic integrity is crucial for cell survival and proliferation, and instability within the genome threatens the faithful propagation of genetic and epigenetic information (1,2). The eukaryotic genome is packaged into chromatin, which is composed of fundamental subunits called nucleosomes, comprising 146 bp of DNA wrapped around an octameric histone complex of a pair each of histones H2A, H2B, H3 and H4 (3).

Eukaryotic chromatin can be divided into two types: the gene-rich, transcriptionally labile 'euchromatin', which bears an open conformation and is preferentially enriched with histone H3 lysine 4 (H3K4) methylation and histone lysine acetylation, and the gene-poor, transcriptionally silenced 'heterochromatin', which is condensed and associated with high H3K9 methylation and reduced lysine acetylation (4–7). Heterochromatin can also be further classified as facultative or constitutive: Facultative heterochromatin is developmentally regulated and conditionally formed via the compaction of transcription-competent chromatin that retains the potential to be transcriptionally activated when appropriate (8), whereas, conversely, constitutive heterochromatin forms over non-coding genomic regions and is often highly enriched with repetitive DNA elements. Constitutive heterochromatin remains compact throughout most of the cell cycle and localises to specialised chromosomal regions, such as the centromere and telomere (9).

The structure of heterochromatin is often studied using fission yeast *Schizosaccharomyces pombe* as a model organism. Resembling higher eukaryotes, fission yeasts contain regional centromeres that comprise central core nu-

*To whom correspondence should be addressed. Tel: +65 6516 5616; Email: bchces@nus.edu.sg

cleosomes incorporating the histone H3 variant CENP-A, and flanking outer repeat regions (*otr*) that bear alternating *dh*/*dg* DNA elements coated with dimethylated H3K9 (H3K9me2) heterochromatin (10,11). The establishment and maintenance of pericentromeric heterochromatin is orchestrated by several complexes, including the H3K9-methylating Clr4 methyltransferase complex (CLRC), the RNA-induced transcriptional silencing (RITS) complex, the RNA-directed RNA polymerase complex (RDRC), and the histone deacetylase Snf2/HDAC-containing repression complex (SHREC) (12–15).

Clr4—the catalytic subunit of CLRC—specifically methylates H3K9 at constitutive heterochromatin regions of the pericentromere, telomere, and mating type locus (16), and creates a binding site for CD-containing proteins, such as Chp1, Chp2, and Swi6 (ortholog of human heterochromatin protein-1 [HP1]) (17–21). Clr4 is itself a CD-containing protein capable of binding H3K9me, which enforces the spreading of heterochromatin over long regions (12). Chp1 is another CD-containing protein that forms part of the RITS complex alongside Argonaut slicer RNase (Ago1) and the adaptor protein Tas3 (13,22). In fission yeast, Ago1 functions in the small interference RNA (siRNA) maturation process in both Dicer-dependent and -independent manners (13,23). Mature siRNA is incorporated into Ago1 to direct the RITS complex to the *otr*, and this is achieved via complementary homology pairing with the transcripts generated from the *otr* (24). The Chp1–H3K9me interaction further anchors the RITS complex at the heterochromatic locus (21) but its affinity can be countered by H3K4 acetylation, which is proposed to enforce dynamic cell cycle regulation of heterochromatin compaction (19). Chp1 and Ago1 are bridged by Tas3; in the absence of Ago1, Tas3 subcomplexes with Chp1 to coordinate RNAi-dependent and -independent transcriptional silencing of sub-telomeric heterochromatin (25).

The RITS complex functions to maintain and establish heterochromatin (24,26). Transcripts from repeat elements located within pericentromeric heterochromatin are generated via RNA polymerase II (RNAPII)-dependent transcription in the S phase of the cell cycle. These transcripts serve as templates for the formation of double-stranded RNA by RDRC and are processed into 21- to 23-nucleotide siRNAs by the RNase III-like Dicer/Dcr1 ribonuclease for incorporation into the RITS complex (21,26–28). RITS is subsequently targeted back to heterochromatic repeat sequences where it recruits the CLRC complex through interaction of Rik1 with Ago1 to facilitate Clr4-dependent H3K9me (12). H3K9me2/3 facilitates the binding of Swi6 and Chp2, which serves as a platform to recruit the SHREC effectors (14,29,30). The recruitment of SHREC results in deacetylation of histones, predominantly at histone H3K14, to limit the accessibility of repeat DNA by RNAPII (14,31).

The dynamic regulation of heterochromatin during the cell cycle permits RNAPII to access the underlying DNA sequence. Most fission yeast cells reside in G2 phase, wherein robust heterochromatin persistently coats the repeat regions. However, beginning in M-phase, the canonical heterochromatin strengthening factors (Swi6 and H3K9me2) are preferentially downregulated to allow RNAPII to access the DNA in early to mid S phase which coincide with the replication of heterochromatin (32–34). As cells traverse this window, heterochromatin is readily reformed in a manner that is dependent on H3K4 acetylation, which coordinates a switch to recruit Swi6 and displace Chp1 (19). However, how heterochromatin 'loosens' at the beginning of S phase and how Swi6 and Chp1 localization is regulated have yet to be clarified.

Here, we show that tyrosine 41 of histone H3 (H3Y41) downregulates silencing of heterochromatin, and phosphorylation of this residue results in the recruitment of Chp1 and displacement of Swi6. We show that there is a preferential enrichment of H3Y41 phosphorylation (H3Y41p) on pericentromeric heterochromatin during the M- to early S phase, yielding new insight into the probable coordination of chromatin dynamics and the regulation of the heterochromatic status during cell cycling.

MATERIALS AND METHODS

Manipulation of fission yeast

Standard procedures of fission yeast handling were employed (35). The spotting assay previously reported was followed (36,37). Briefly, strains were inoculated in YEA (3% glucose, 0.5% yeast extract, 75 mg/l adenine) broth and grown overnight to mid-log phase. Cells were adjusted to a concentration of 1×10^7 cells/ml, from which five steps of a ten-fold serial dilution were performed. Each cell culture (3 μl) was spotted onto plates to test cellular sensitivity to DNA damage-generating drugs. Strains employed for this study are listed in Supplementary Table S1.

RNA sequencing and data analysis

Cell pellets harvested from mid-log phase cultures were homogenised using glass beads (0.5 mm; BioSpec, Bartlesville, OK) and a Fastprep homogenizer (MP Biomedicals, Switzerland). RNA samples were extracted using TRIzol (Thermo Scientific, Waltham, MA) and purified by phenol:chloroform:isoamyl alcohol (25:24:1) (PCI) (Nacalai Tesque, Kyoto, Japan) extraction thrice. Total RNA (50 μg) was treated with DNase I (Thermo Scientific) in the manufacturer-supplied buffer following the manufacturer's protocol. DNase-treated RNA samples were then purified using an equal volume of PCI thrice and then precipitated in ethanol overnight and resuspended in ultrapure water (Nacalai Tesque). RNA-seq and primary data analyses were supplied by BGI (Shenzhen, China) using an Illumina HiSeqTM 2000 platform (Illumina, San Diego, CA). RNA reads were mapped to the *S. pombe* genome (ASM294v2.25) using Novoalign (http://www.novacraft.com) to generate the SAM/BAM files. Expression levels of the genes were then determined based on the BAM files by HTseq (38). Normalization of the expression data among all of the samples was performed using the total mappable counts. Differentially expressed genes (DEGs) were then determined based on normalised gene expression data using a fold change cut-off of 2. The DEGs were further clustered and visualised using heat maps. The GEO accession code of RNA sequencing data is GSE102125.

Reverse transcription PCR (RT-PCR)

RNA extraction procedures were carried out as described for RNA sequencing. DNase-treated RNA was reverse transcribed into cDNA using a Onestep-RT Kit (Qiagen, Limburg, Netherlands) as per the manufacturer's instructions.

Quantitative PCR (qPCR)

PCR amplification was conducted using a StepOne real time PCR system (Applied Biosystems, Thermo Scientific) using iTaq Universal SYBR Green Supermix (Bio-Rad) following manufacturer's instructions. Primer sequences are listed in Supplementary Table S2.

Western blot and antibodies

A previously published western blotting procedure was followed (39). Antibodies used for this study were H3Y41p (Merck Millipore, Billerica, MA, 1:100), Cdc2 (Santa Cruz Biotechnology, Dallas, TX, 1:500), H2A (Merck Millipore, 1:200), H2B (Merck Millipore, 1:200), H3 (Merck Millipore, 1:500), H4 (Merck Millipore, 1:500), HA (Roche Applied Science, 1:500), Swi6 (Abcam, UK, 1:1000), Chp1 (Abcam, 1:100), GFP (Roche Applied Science, 1:500), FLAG (Wako, Japan, 1:500). Western blot chemiluminescence was detected using ImageQuant LAS4000 imager, and protein band intensities were measured using ImageQuant TL software (GE Healthcare, Little Chalfont, UK). Protein levels were calculated by normalising band intensity against control expression in the same run.

Cell cycle synchronization

Exponentially growing *cdc25-22* cells were synchronised to G2/M phase by 4.5 h incubation at 36°C. To release from the G2/M phase, *cdc25-22* cells were transferred to 26°C. S-phase cells were obtained by treatment with 15 mM HU for 4 h at 30°C. Cells were washed with sterile water five times to remove HU before releasing into new media.

Chromatin immunoprecipitation (ChIP)

Schizosaccharomyces pombe cell cultures were fixed with 3% paraformaldehyde (PFA) (Sigma-Aldrich, St Louis, MO) for 30 min, then quenched with 0.2 M glycine. For non-histone targets, cells were fixed with 10 mM dimethyl adipimidate (DMA) (Thermo Scientific) for 45 min at room temperature after PFA fixation. Cells were then washed with PBS thrice. ChIP was conducted as previously described (33,39). Relative fold enrichment was calculated by the ΔΔCt method, whereby NDR or *act1* was used as internal control and further titrated from the whole cell extract (WCE) or histone H3 immunoprecipitant as backgrounds.

Micrococcal nuclease digestion

Cells were cultured to mid-log phase at 30°C and then harvested. Cells were washed with and resuspended in 500 μl CES buffer (50 mM citric acid pH 5.6, 40 mM EDTA pH 8.0, 1.2 M sorbitol, 10 mM β-mercaptoethanol). Cell suspensions were then combined with 0.5 mg Zymolyase-100T (Seikagaku, Tokyo, Japan) to digest cell walls at 30°C for up to 45 min. Spheroplasts were washed with ice-cold 1.2 M sorbitol and resuspended in 800 μl NP-S buffer (1.2 M sorbitol, 10 mM $CaCl_2$, 100 mM NaCl, 1 mM EDTA pH 8.0, 14 mM β-mercaptoethanol, 50 mM Tris-HCl pH 8.0, 0.075% NP-40, 5 mM spermidine, 0.1 mM PMSF, 1% protease inhibitor cocktail [Sigma Aldrich]). Each sample was then divided into four equal aliquots, and each mixed with 300 μl of NP-S buffer. Samples were then digested with 3.8 U of MNase (M0247S; New England Biolabs, Ipswich, MA) for 0, 3, 6 or 12 min at 37°C. MNase activity was terminated by the addition of 50 mM EDTA pH 8.0 and 0.2% SDS. Samples were then incubated with 0.2 mg/ml proteinase K (New England Biolabs) and 10 μg/ml RNase A at 65°C overnight. Digested DNA was purified by PCI (Nacarai Tesque, Japan) extraction and precipitated with ethanol. Purified DNA was separated on agarose gels and post-stained with ethidium bromide (Life Technologies).

Peptide pull-down

For each strain, 1 l of mid-log phase cell culture was harvested, and cell extracts were prepared in HB buffer (25 mM Tris–HCl pH 7.5, 60 mM β-glycerophosphate, 15 mM *p*-nitrophenyl phosphate, 0.1 mM NaF, 0.5 mM Na-orthovanadate, 0.5% Triton X-100, 15 mM EDTA, 15 mM $MgCl_2$) supplemented with 1 mM DTT and 1 mM PMSF. Samples were homogenized using glass bead disruption in a Fastprep homogenizer (MP Biomedicals, Switzerland). The extracts were then centrifuged at 14 000 rpm at 4°C to remove the insoluble portion of the lysate, and then precleared using streptavidin agarose beads (Thermo Scientific) rotating at 4°C for 1 h. After removing the beads, 100 μl of whole cell extract (WCE) was removed and stored in a separate tube for western blotting.

The remaining sample was then divided equally into two tubes and incubated for 1 h with unmodified or H3Y41p peptides (Mimotopes, Victoria, Australia) (Supplementary Table S3), which had been pre-incubated with streptavidin agarose beads by rotating in 4°C for 1 h. Peptide-beads were collected and washed seven times with HB buffer. Proteins that bound to the peptides were eluted and denatured in sampling buffer for western blotting.

For testing the interaction between K9me2 and H3Y41p, 25 μg of H3K9me2 peptides were mixed with streptavidin agarose for 1 h in HB buffer, washed, and then mixed with the same amount of H3Y41p or H3Y41F peptides for another 1 h. Beads bound with the two peptides were then incubated with cell extracts.

Recombinant protein production

Target genes of interest from genomic DNA were amplified by PCR using Phusion DNA polymerase (Thermo Scientific), precipitated with ethanol, digested with restriction enzymes, and then ligated into the pET32a expression vector (Novagen, Millipore). Sequencing (1st Base Sequencing, Singapore) was used to ensure correct amplification of the genes. Swi6 recombinant protein expression was induced in BL21 cells in LB media containing 100 μg/ml

carbenicillin and 1 mM IPTG (Thermo-Scientific) at 30°C for 4.5 h. Induction of Chp1 protein expression was performed in TB media with 1 mM IPTG and 100 μg/ml carbenicillin at 20°C for 24 h. To purify the recombinant proteins, bacterial cells were lysed in Ni-NTA lysis buffer (50 mM NaH_2PO_4, 300 mM NaCl, pH 8.0, 1 mg/ml Lysozyme [Sigma-Aldrich], 10 mg/ml RNase A [Roche], 5 mg/ml DNase I [Roche], 10 mM Imidazole [Sigma-Aldrich]) for 30 min on ice, and subjected to two rounds of sonication for 30 s followed by a 2-min rest interval on ice. Samples were then centrifuged at 9000 × g at 4°C for 30 min. The cleared supernatants were then loaded onto Ni-NTA spin columns (31314, Qiagen) and eluted as per the manufacturer's protocol. The eluted samples were concentrated using a 10-kDa MW cut-off protein concentrator column (Pierce, Thermo Scientific) and buffer exchanged with a buffer containing 50 mM Tris–HCl pH 7.5 and 200 mM NaCl.

Bio-layer interferometry (BLI) binding assay

Binding assays for H3K9me2 (K9me2), H3Y41F (Y41F), or H3Y41p (Y41p) peptides with the Swi6 protein were performed using a FortéBIO Octet RED 96 instrument (PALL Corporation, New York). The BLI assays were carried out in a buffer containing 20 mM PBS pH 7.4, 100 mM NaCl, 0.1% BSA, 0.1% Tween-20 at 30°C. The biotinylated peptides (5 μg/ml) were immobilized onto streptavidin-coated biosensors (PALL) for 600 s. Using different concentrations of the Swi6 protein, binding was permitted for 120 s followed by a dissociation time of 300 s. Data were analysed using in-house Octet software, v 9.0.0.14 (PALL). Global analyses of the data were performed by using nonlinear regression fitting to derive the dissociation constants.

RESULTS

Construction of a loss-of-function H3Y41 mutant

H3Y41 lies at the junction of the flexible N-terminal tail and the αN helix of the histone fold domain of histone H3 (Supplementary Figure S1A), close to the dyad axis where DNA enters and leaves the nucleosome (Supplementary Figure S1B). H3Y41 can be phosphorylated by ectopic JAK2 in erythroid leukaemia cells, and this transcriptionally induces oncogenes by antagonising binding of the HP1α protein to chromatin (40,41). Phosphorylation of Y41 is thought to modulate the DNA–histone octamer to induce chromatin unwrapping and increase chromatin accessibility (42). To assess the *in vivo* genome-wide role of H3Y41p, we constructed a mutant in which all three copies of histone H3 genes on the fission yeast genome were replaced with the loss-of-function allele of Y41F (Supplementary Figure S2A). The resultant strain endogenously expressed the mutant form of histone H3, with the Y41 residue replaced by the non-phosphorylatable phenylalanine. Phenylalanine lacks the hydroxyl group on which the phosphoryl group attaches but is otherwise structurally like tyrosine (Supplementary Figure S2B). This mutant strain was attained through several levels of genetic crosses to progressively replace the wild-type (WT) histone H3 genes with the F mutant (Supplementary Figure S2C).

We first confirmed that the Y41F mutation was correctly incorporated into the three histone H3 genes via direct sequencing and then checked by immunoblotting that this mutation did not destabilise the histone H3 protein or other canonical histones (Supplementary Figure S3A). Micrococcal nuclease cleavage assay revealed a similar ladder pattern between Y41F and WT, suggesting that the site-directed mutagenesis did not grossly alter global chromatin compaction (Supplementary Figure S3B). The growth rate of the mutant cells over a range of temperatures (20–36°C) was comparable with that of the WT, consistent with a lack of chromatin perturbation imposed by the Y41F substitution (Supplementary Figure S4A–C). This was further confirmed via phenotypic quantification of cells at different stages of the cell cycle (Supplementary Figure S4D).

Y41F hosts aberrant transcriptional silencing at heterochromatic regions

To ascertain the effect of the Y41F mutation on the genome, we assessed the global transcription pattern of the Y41F mutant with respect to the WT using whole-genome RNA sequencing. Approximately 50 million reads were sequenced and mapped onto the three fission yeast chromosomes. Genes with a variation in expression above 2-fold were considered as differentially expressed genes (DEGs). Overall, the transcription profiles were similar between WT and Y41F on the three chromosomes (Figure 1A). However, 34 genes (0.66% of whole transcriptome) showed differential regulation, 29 of which (0.56% of whole transcriptome) showed at least a 2-fold upregulation in expression as compared with WT (Figure 1B and C). While these genes were not enriched in a particular ontological group, their upregulation may indicate a repressive function of H3Y41p. Additionally, five genes were downregulated in the Y41F mutant: two *Tf* retrotransposons (*tf2–7*, *tf2–8*) and three uncharacterised genes (*SPAC212.01c*, *SPAC977.05c*, *SPAC750.08c*). These uncharacterised genes are all located within the subtelomeric region, situated within 60 kb from the telomere (Figure 1C). Real time PCR was conducted on several differentially expressed genes to confirm the RNA sequencing results (Supplementary Figure S5A. *SPAC977.05c*, B. *SPAC750.08c* and C: *shu1*).

From our RNA sequencing data, we hypothesized that Y41F may affect chromatin compaction at sub-telomeres, which are wrapped in heterochromatin (7,33,43). The subtelomeric region encompasses a *dh*-like heterochromatin-nucleation repeat element that is nested in two subtelomere-situated helicase genes (*tlh1* and *tlh2*) on chromosomes 1 and 2, respectively (7,43). We detected a low level of transcription originating from these elements in WT that was repressed in the Y41F mutant. Repression to a lesser extent was observed at the centromeric *dh* sequences within the heterochromatic repeats owing to the tightly repressed transcription therein (Figure 1D). These observations were reproducible using RT-PCR, noting a 2.74-fold repression in the expression of subtelomeric elements and 1.44-fold repression at centromeric *dh* elements relative to that in WT ($P < 0.05$, Figure 1E). Considering the low expression of transcription originating from centromeric heterochromatin in WT, which may confound our interpretation, we

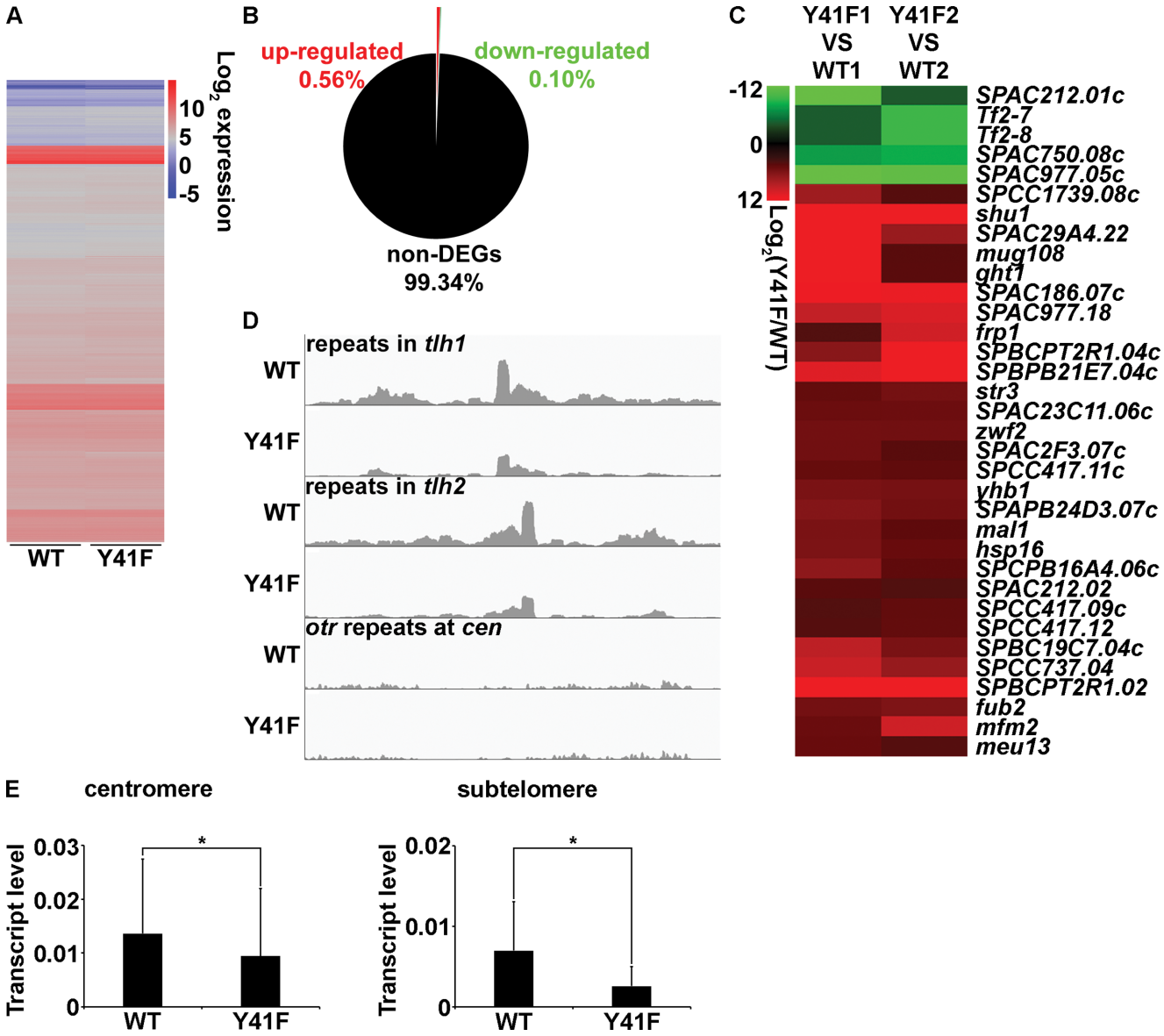

Figure 1. Whole-genome RNA sequencing reveals impact of H3Y41 loss-of-function mutant on centromeric and subtelomeric heterochromatin. (**A**) Genome-wide gene expression profiles in WT and Y41F mutant cells, as tested by RNA sequencing. Color code on top right depicts gene expression level. (**B**) Proportion of differentially (DEGs) and non-differentially (non-DEGs) expressed genes in the Y41F mutant. Values were determined from two independent sets of RNA sequencing results. (**C**) List of DEGs in Y41F. Gene list represents the overlap between the two RNA sequencing replicates. Colour code listed on top left depicts the difference in expression level. (**D**) RNA sequencing reads at subtelomeric *tlh1* and *tlh2*, and *otr* pericentromeric repeats of chromosome 2. (**E**) RT-qPCR to detect transcripts derived from heterochromatic *dh* loci at the centromeric and subtelomeric regions in WT and Y41F strains relative to the *act1*internal control. Bar graphs depict mean ± S.D., $n = 10$. P, *P*-value of pairwise two-sided *t*-test. *, $P < 0.05$.

concomitantly disrupted Chp1 (*Δchp1*) in the Y41F background. Chp1 is a subunit of the RITS complex, which is essential for establishing and maintaining heterochromatic silencing at the centromere, and others have reported that disrupting Chp1 function can increase the level of transcript de-repression from the *dh* elements at centromeric and subtelomeric regions (13,21).

We found that *Δchp1* exhibited approximately 9.60- and 8.74-fold upregulation of transcripts derived from subtelomeric *dh* (*subtel-dh*) and centromeric *dh* (*cen-dh*) elements, respectively. Interestingly, at both heterochromatic domains, this transcript upregulation was partially suppressed (56.00% and 26.02%) when H3Y41 was also mutated (Figure 2A). A similar suppressive effect by Y41F was also observed on the de-repressed transcript after disrupting Clr4 (*Δclr4*), the catalytic subunit of the CLRC complex (Figure 2B), as well as with the null mutation of Ago1 (*Δago1*); albeit, this was only at the centromeric *dh* locus (*cen-dh*) and not at the *dh* element at the subtelomere (*subtel-dh*) of *Δago1* (Figure 2C). Taken together, these observations confirm that H3Y41 integrity is important for heterochromatin transcription, and that disrupting this residue rescues the de-repression of *dh* transcription as-

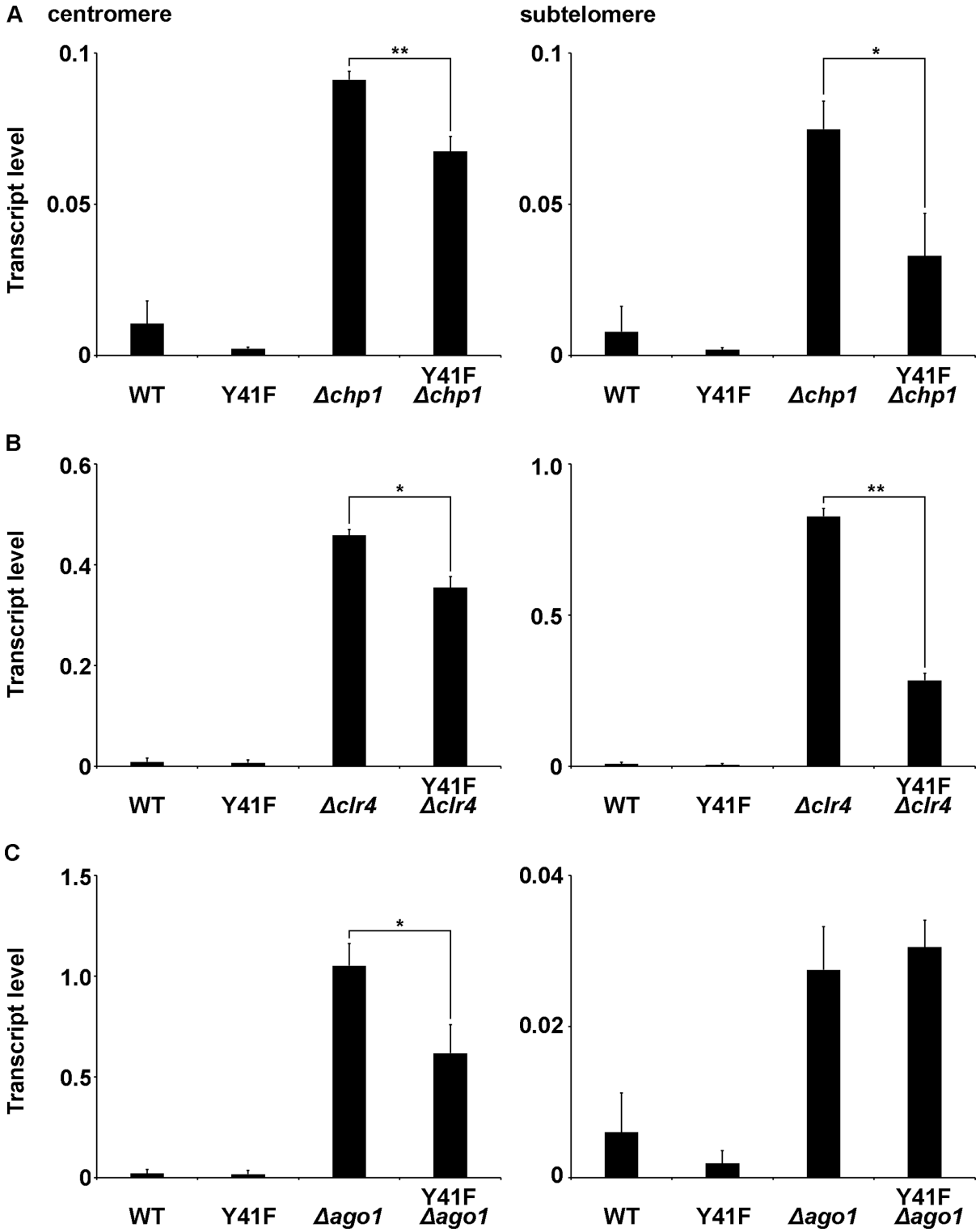

Figure 2. Loss of transcriptional silencing at heterochromatic loci in RNAi and *Δclr4* mutants can be ameliorated by Y41F mutation. RT-qPCR was performed to detect the transcripts derived from centromeric and subtelomeric repeats in the indicated mutant strains relative to internal control. Strains tested were (**A**) WT, Y41F, *Δchp1* and Y41F*Δchp1*, (**B**) WT, Y41F, *Δclr4* and Y41F*Δclr4* and (**C**) WT, Y41F, *Δago1* and Y41F*Δago1* mutants. *Δ* indicates gene deletion. *act1* transcripts were used as an internal control. Bar graphs depict mean ± S.D., $n = 3$–4. P, *P*-value of pairwise two-sided *t*-test. $*P < 0.05$; $**P < 0.01$.

sociated with heterochromatic disruption, probably with a position-specific effect.

To test whether the silencing effect of the Y41F mutant resulted from a change in the heterochromatin hallmark H3K9 methylation, we assessed H3K9me2 and H3K9ac levels in the Y41F mutant by ChIP. Y41F contained comparable levels of dimethylated (Figure 3A) and acetylated H3K9 as that in the WT (Figure 3B) at both the centromeric and sub-telomeric heterochromatin, suggesting that the silencing effect associated with the Y41F mutant can occur without altering the H3K9 methylation status. Using ChIP of H4K16ac—the deacetylation of which is crucial for heterochromatin formation (44,45)—we found that the Y41F mutant maintained a similar level of this histone acetylation as the WT at both centromeric and sub-telomeric heterochromatin (Figure 3C).

H3Y41p differentially regulates localization of CD proteins at heterochromatic regions

To further investigate how H3Y41p confers its anti-silencing effect, we interrogated whether H3Y41p regulates the binding of heterochromatin-associated proteins. We first tested the binding of the fission yeast HP1 protein Swi6 to a biotinylated histone H3 N-terminal peptide harbouring a phosphorylated Y41 (Y41p). We incubated both Y41F and Y41p peptides with WT cell extracts to affinity precipitate endogenously expressed Swi6, and observed a preferential association of Swi6 with Y41F over Y41p peptide, suggesting that phosphorylation of H3Y41 counteracts the interaction of Swi6 with histone H3 (Supplementary Figure S6A). To observe the effect of Y41p on H3K9me2-bound Swi6, we repeated the peptide pull down experiment in the presence of a H3K9me2 peptide, on which Swi6 was bound (16). We found that the interaction between endogenously expressed Swi6 and the Y41F peptide was reduced by 37.32% when Y41 was phosphorylated ($P < 0.05$) (Figure 4A).

We further employed bimolecular binding kinetic assays to show that bacterially produced recombinant Swi6 exhibited a dose-dependent direct binding to the histone H3 N-terminal sequence hosting the Y41F mutation (Figure 4B, top, $K_D = 57.2 \pm 1.41$ nM, $R^2 = 0.9833$). This interaction was reminiscent of the interaction of the recombinant Swi6 protein with the H3K9me2 peptide (Figure 4B, bottom, $K_D = 62.8 \pm 1.76$ nM, $R^2 = 0.9742$); similar binding was not observed for recombinant Swi6 and the Y41p peptide (Figure 4B, middle). Collectively, these results strongly suggest that Swi6 can bind directly to the histone H3 N-terminus and that this association is counteracted by phosphorylation of H3Y41.

Next, we tested whether the exclusion of Swi6 binding by H3Y41p may also be recapitulated *in vivo*. We performed ChIP of the endogenous Swi6 protein in WT and Y41F backgrounds. Consistent with the pull-down experiment, the Y41F mutant exhibited 34.56% and 24.24% increases in Swi6 localization at the *dh* sequences of centromeric and sub-telomeric heterochromatic regions, respectively (Figure 4C). Further immunoblot analysis confirmed that the observed increases were not due to an upregulation in the Swi6 protein level in the Y41F cells, which was similar to that of WT cells (Figure 4D).

Y41F was shown to partially suppress the de-repression of heterochromatin transcription that arose from the absence of Chp1 (Figure 2A). Like Swi6, Chp1 protein also contains a CD motif that can bind to methylated H3K9 (13). Thus, we next investigated whether H3Y41p can also counteract Chp1 binding to histone H3 by repeating the peptide pull-down and ChIP experiments conducted for Swi6 (Figure 4). To our surprise, contrary to the experiments with Swi6, we detected a 2.62-fold increase in Chp1 association with the phosphorylated histone H3 peptide as compared with the unmodified peptide, suggesting that H3Y41p recruits Chp1 (Figure 5A). This observation was confirmed using a strain expressing a GFP-tagged Chp1 (Supplementary Figure 6B). Consistent with this finding, the localization of Chp1 protein on centromeric heterochromatin was reduced by 42.30% in the Y41F mutant (WT was 1.73-fold of Y41F), and 55.62% on subtelomeric heterochromatin (Figure 5B); Chp1 protein levels were similar between the WT and Y41F strains (Figure 5C).

Fission yeast hosts another Swi6-like heterochromatin protein, Chp2, which shares an overlapping role with Swi6; albeit, it is expressed at a lower level (46). In view of the opposing effect of H3Y41p on Swi6 and Chp1 localization, we expected that Chp2 would be more like Swi6 than Chp1 in its interaction with H3Y41p. We checked this hypothesis using ChIP with a Chp2-FLAG fusion protein in WT versus Y41F strains. Contrary to our expectation, peptide pull-down experiments showed a similar level of association for Chp2-FLAG with both the H3Y41p and Y41F peptides, suggesting that H3Y41p does not directly change the interaction of Chp2-FLAG with heterochromatin (Supplementary Figure S7A). This aside, the ChIP results did show a ∼2-fold reduction in the localization of Chp2-FLAG at both centromeric (2.22-fold) and sub-telomeric (2.21-fold) heterochromatin *in vivo* in the Y41F strain relative to that of WT (Supplementary Figure S7B). As with Swi6 and Chp1, Chp2 protein levels were unaffected by the Y41F mutation (Supplementary Figure S7C), indicating that the observed changes were due to an altered localization of the Chp2 protein, probably influenced by the local chromatin context. Heterochromatin proteins Swi6, Chp1 and Chp2 are recruited to the heterochromatin loci through an interaction between their CD motifs and methylated H3K9 (16,18,46). Our observations thus reveal a novel mechanism that functions in parallel with H3K9 methylation to regulate the localization of these CD-containing proteins.

Cell cycle regulation of H3Y41p at centromeric heterochromatin

The interaction of H3Y41p with Swi6 and Chp1 in conjunction with the effect of Y41F on heterochromatic silencing indicated that H3Y41p localises to the heterochromatin loci. To confirm this, we performed ChIP to detect H3Y41p at the heterochromatin loci. In asynchronised cell cultures, we observed a low enrichment (2.04-fold) over the Y41F control on centromeric heterochromatin regions (Supplementary Figure S8), which suggested that H3Y41p may be cell-cycle regulated.

We next prepared extracts to perform ChIP to assess H3Y41p level at centromeric heterochromatin. Synchro-

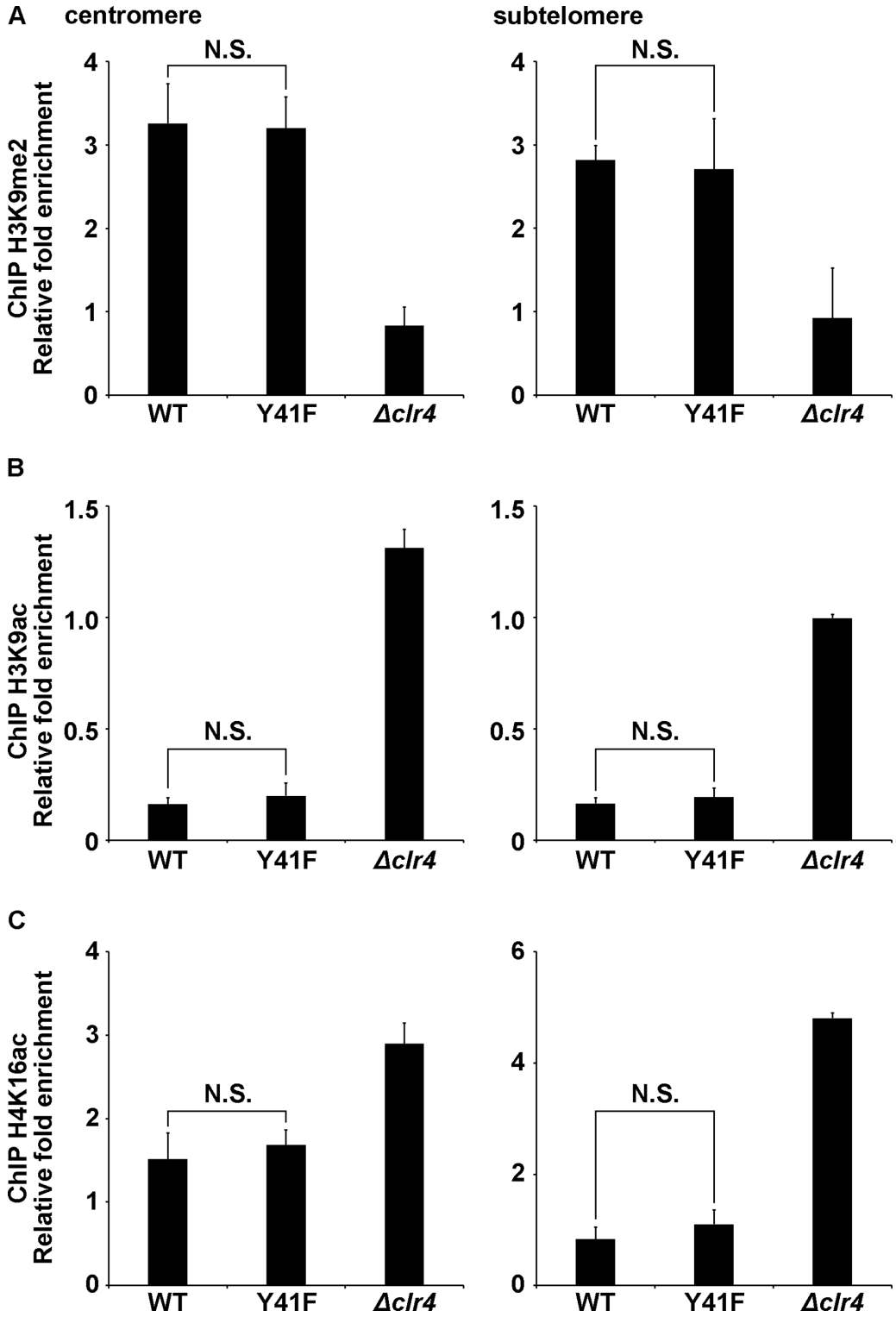

Figure 3. Post-translational modifications on H3K9 and histone acetylation levels at heterochromatic loci are not affected by H3Y41 loss of function. ChIP was performed to detect the levels of (**A**) H3K9me2, (**B**) H3K9ac and (**C**) H4K16ac at centromeric (left), and subtelomeric (right) repeats in WT, Y41F and *Δclr4* mutants. Graphs show relative fold enrichment compared with *act1* and the data are normalised to whole cell extract (WCE). Bar, standard deviation (S.D.) derived from three biological repeats. N.S., not significant using pairwise two-sided *t*-test.

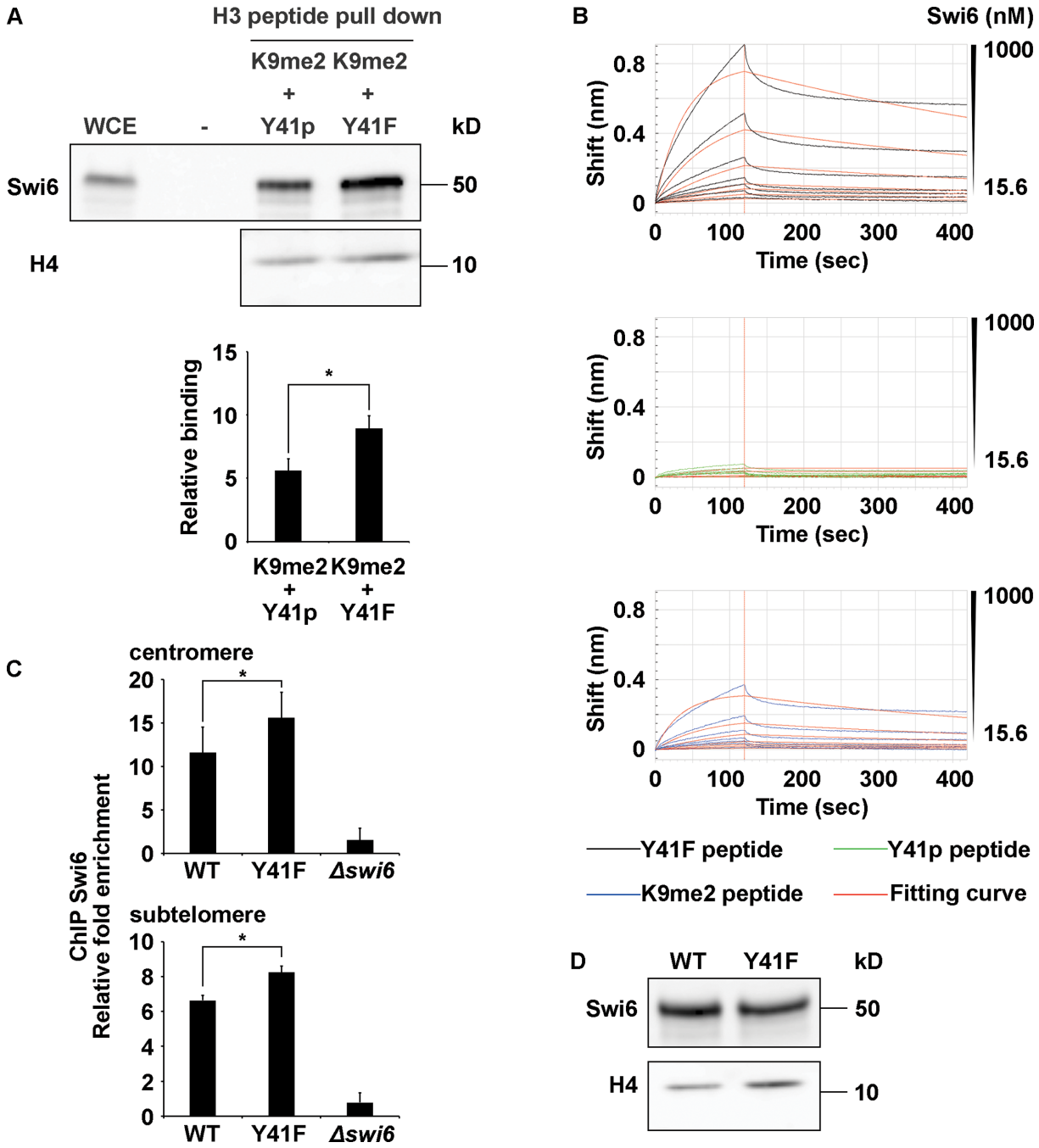

Figure 4. H3Y41p excludes Swi6 from heterochromatin regions. (**A**) Peptide pull-down assays were performed on whole cell extracts (WCE) using H3Y41p (Y41p) or Y41F peptides, incubated with K9me2 peptide, as described in the Materials and Methods. Swi6 binding was quantified relative to histone H4. Graph (bottom) depicts the mean ± S.D., $n = 3$. P, P-value of pairwise two-sided t-test. *$P < 0.05$. (**B**) Bio-Layer Interferometry (BLI) binding assay of Swi6 recombinant protein with Y41F peptide (top), Y41p peptide (middle) and K9me2 peptide (bottom). (**C**) ChIP of Swi6 on centromeric and subtelomeric repeats in WT, Y41F, and *Δswi6*. Fold enrichment of Swi6 was relative to *act1* over that in WCEs. Mean ± S.D. are shown, $n = 4$. P, P-value of pairwise two-sided t-test. *$P < 0.05$. (**D**) Western blot of Swi6 protein levels in WT and Y41F context. Histone H4 serves as a loading control.

nised WT cells at G1/S phase incubated with 15 mM HU were released synchronously into the cell cycle to collect samples at regular (30-min) time intervals. Relative enrichment of H3Y41p on centromeric heterochromatin was determined by normalising to signals associated with a nucleosome-depleted region (47); Y41F strain was included as a negative control. Interestingly, we detected a preferential enrichment at two time points at which the septation index—which peaks in mid-S phase (33)—started to increase (Figure 6, middle). A similar profile was observed when the ChIP signals of Y41p were normalised to that of histone H3, showing that the observed H3Y41p enrichment was not simply due to a general change in the overall level of histone H3 (Supplementary Figure S9).

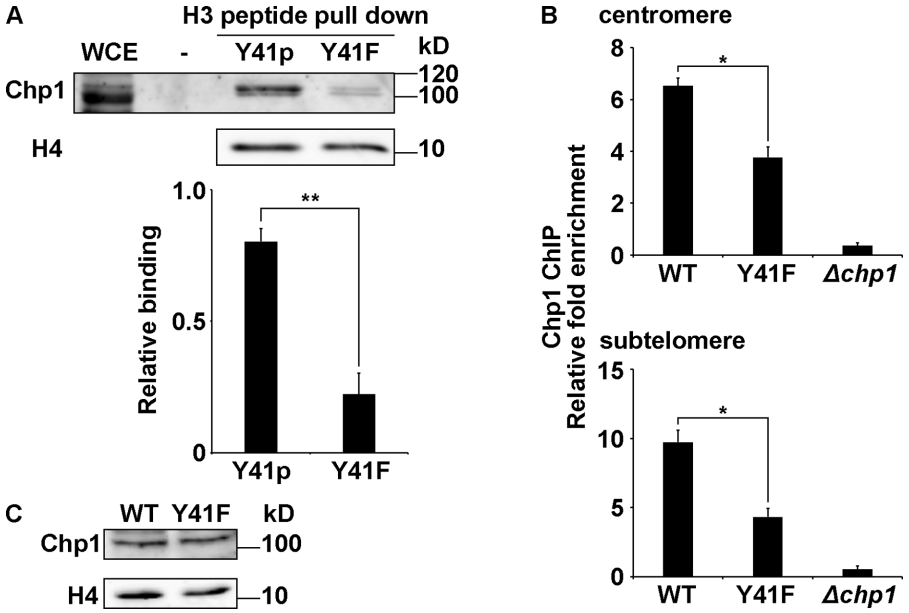

Figure 5. H3Y41p enhances the recruitment of Chp1 to centromeric heterochromatin. (**A**) Peptide pull-down assay was performed on cell extracts using unmodified (Y41F) or H3Y41 phosphorylated (Y41p) peptides. Histone H4 serves as a loading control. WCE, whole cell extract. Graphs (bottom) show the level of protein affinity purified by the corresponding peptides. Mean ± S.D. are shown, $n = 3$. P, P-value of pairwise two-sided t-test. $^{**}P < 0.01$. (**B**) ChIP was performed to quantify the binding of Chp1 on centromeric and subtelomeric repeats in WT, Y41F and *Δchp1* strains. Fold enrichment of Chp1 was relative to *act1* over that in whole cell extracts. Mean ± S.D. are shown, $n = 3$. P, P-value of pairwise two-sided t-test. $^{*}P < 0.05$. (**C**) Western blot demonstrating Chp1 protein levels in WT and Y41F strains. Histone H4 serves as a loading control.

Preferential enrichment of H3Y41p was detected for three consecutive cell cycles at 0.5 h (relative fold enrichment, 4.78; $P < 0.01$), when the cells were just released from the G1/S block (Figure 6), as well as at 2–2.5 h (relative fold enrichment, 10.23 and 7.79; $P < 0.05$) and at 3.5 h (relative fold enrichment, 2.53; $P < 0.05$; this lower enrichment is probably due to a loss of cell cycle synchrony). Similar enrichment was also observed in synchronised *cdc25–22* cell cultures collected after releasing from the G2/M phase (Supplementary Figure S10), and at two other heterochromatic sequences located on all three chromosomes (Supplementary Figure S11A-B, Cen-FO7064 on chromosome [Chr] II and III; S11C-D, Cen-MT2012 on Chr I and III and S11E-F, Cen-EG2005 on Chr I and II, normalized to qNDR [left] and *act1* [qAct1, right]). These results suggest that H3Y41 is preferentially phosphorylated in nucleosomes encompassing the heterochromatic sequences at the centromere during early S phase of the cell cycle and that it probably regulates heterochromatin transcription by switching Swi6 and Chp1 at this stage. Through ChIP, we also found that the increased centromeric localization of Chp1 correlated with the upregulation of H3Y41p in synchronized WT cells (Supplementary Figure S12).

To delineate the phase of H3Y41p preferential enrichment, we also quantified the cell cycle fluctuation of *cdc15*$^{+}$ and *cdc22*$^{+}$, which peak in M- and G1- to S-phases, respectively (48). We observed an overlap of H3Y41p enrichment at the time at which *cdc15*$^{+}$ and *cdc22*$^{+}$ peaked (Figure 6, Supplementary Figure S10). Both synchronization experiments showed fluctuations in *cdc15*$^{+}$ and *cdc22*$^{+}$ in the first cell cycle, presumably a consequence of the synchronization treatment. Even so, peaks in H3Y41p expression were still observed; albeit, they had slightly shifted as compared with the results of the second cell cycle. H3Y41p enrichment was reduced by the third cell cycle, likely due to the loss of cell synchrony, as evident from the low periodicity of the *cdc15*$^{+}$ and *cdc22*$^{+}$ transcripts (Figure 6, bottom). Taken together, nucleosomes in the centromeric heterochromatin are phosphorylated on Y41 preferentially from late M- until the early S-phase, coinciding with the phases at which Swi6 localization is downregulated on centromeric heterochromatin (33).

Loss of function of H3Y41 enhanced tolerance of RNAi defective mutants to HU

In fission yeast, heterochromatin persistently coats the repeat region in the G2 phase; however, previous studies show that a window exists during S phase when heterochromatin is momentarily destabilised to permit the transcription of the underlying repeat DNA for the S phase-coupled inheritance of the silenced state (33,34). In this brief window, transcription and DNA replication co-occur within the same stretch of heterochromatic domain (33,49). If not properly regulated, the genome can become unstable; for example, from collision between the RNA and DNA polymerases. Previous studies have shown that RNA interference (RNAi) machinery—among other factors—helps to prevent this potential conflict (50–52).

Several groups have shown that RNAi mutants exhibit hypersensitivity to HU, a drug that stalls the replication fork in S phase (53,54). Using a serial dilution assay, we observed HU hypersensitivity in cells bearing mutations in several genes that encode for factors that function intimately with RNAi machinery during heterochromatin establish-

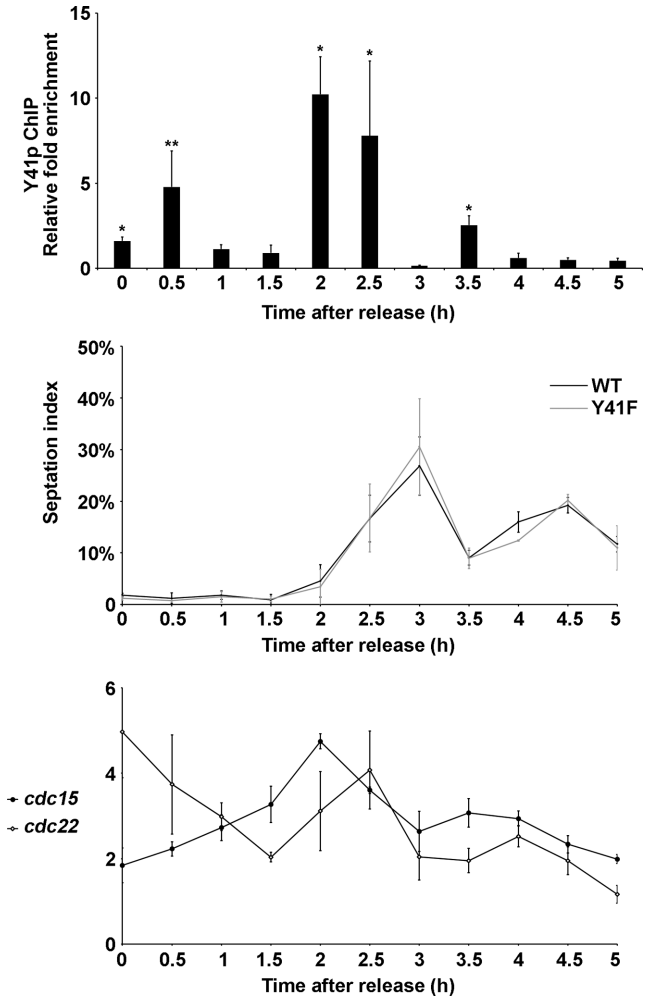

Figure 6. H3Y41p is enriched in M-S-phase cells. Top, H3Y41p (Y41p) levels at centromeric repeats (*cen*) in HU-synchronised cells. Fold enrichment of Y41p relative to a nucleosome-depleted region (NDR) over that in whole cell extract. Synchronised Y41F was used as a negative control. Relative fold enrichment values were normalised to that of Y41F at each time point. Bar graph depict mean ± S.D., $n = 3$. P, *P*-value of pairwise two-sided *t*-test. $*P < 0.05$; $**P < 0.01$. Middle, septation index of cells synchronised with HU. Error bars indicate S.D. of three independent block-release experiments. Bottom, RT-PCR of *cdc15* and *cdc22* expression level relative to *act1*, Error bars, S.D. of three independent experiments.

ment in S phase: *Δrik1, Δcid12,* and *Δchp1*. Comparatively, deletion of *swi6* and *clr3*, which encode for proteins that function in heterochromatin maintenance (33,55), induced a milder or no hypersensitivity to HU (Supplementary Figure S13A). We detected a much higher level of de-repression of *cen-dh* transcripts from the *Δrik1, Δcid12* and *Δchp1* mutants than the *Δswi6* and *Δclr3* mutants (Supplementary Figure S13B). This consistency among the mutants in their respective groups indicates that centromeric transcriptional derepression and HU sensitivity may be linked to the instability that arises during S phase when RNAPII is involved in increased collisions with the replication machinery (51). Interestingly, a disruption of H3Y41 in two of the RNAi mutants, *Δago1* and *Δchp1*—which reduced the upregulation of *cen-dh* transcripts (Figure 2)—strongly suppressed HU hypersensitivity of these mutants (Figure 7A). Collectively, these findings suggest that H3Y41 may also be involved in coordinating heterochromatin transcription and replication during S phase.

DISCUSSION

H3Y41 was initially characterised to be ectopically phosphorylated by the overproduction of JAK2 in human leukemic cells on a transcriptionally silenced oncogene (40). Here, we show that H3Y41p exerts an important role in regulating the transcriptional silencing of constitutive heterochromatic domains at centromeres and subtelomeres in fission yeast. H3Y41p imposes a differential effect on CD-containing proteins, enhancing the localization of Chp1 and Chp2 while affecting the delocalization of Swi6 in a manner that is independent of canonical heterochromatin-regulating histone H3K9 methylation. We suggest that H3Y41p hosts an anti-silencing effect to control the transcription of non-coding DNA repeats under heterochromatin and regulate the compaction of these heterochromatic loci.

H3Y41 occupies a strategic location at the junction between the N-terminal tail and the histone fold domain of histone H3, and lies at the dyad axis of the nucleosome at the site where DNA enters and exits the nucleosome (Supplementary Figure S1B). This region of the nucleosome is highly basic, populated by numerous positively charged amino acids. 3D nucleosome modelling posits that the side chain of H3Y41 protrudes into the DNA minor groove (Supplementary Figure S1B) (56), thus positioning H3Y41 at a critical site to modulate DNA compression against the nucleosome surface. The attachment of a negatively charged phosphoryl moiety on this residue would not only impose a steric clash with the DNA but also modulate DNA–octamer contact owing to electrostatic repulsion with the negatively charged DNA backbone. The net result of these effects would induce a partial unwrapping of the DNA at this location. Indeed, nucleosome unwrapping *in vitro* can improve DNA accessibility to some transcription factors on reconstituted nucleosomes with the histone H3Y41p (42).

Previous studies in human cell lines have found that HP1α-bound, silenced chromatin regions are enriched with methylated H3K9 but lack H3Y41 phosphorylation (40). Furthermore, inhibiting JAK2 can abolish H3Y41 phosphorylation, correlated with an upregulation in H3K9 methylation, indicating an inverse relationship between H3K9me and H3Y41p (57). Here, using a loss-of-function Y41F mutant, we show a similar relationship between Swi6—a HP1 fission yeast ortholog—and H3Y41p. However, we found that the net effect of H3Y41 phosphorylation on Swi6 localization was functionally distinct from H3K9 methylation. In addition, the regulatory role of H3Y41p on proteins that control transcriptional silencing appears to be more complicated than originally expected, as H3Y41p induces differential binding of CD-containing proteins, which all contribute to transcriptional silencing (58). We thus expect that transcriptional silencing outcomes will be dependent upon the presence of other histone modifications and the context in which H3Y41p is introduced. Since fission yeast mostly reside in the G2 phase—preferentially relying on Swi6 for transcriptional silencing—mutation of the tyro-

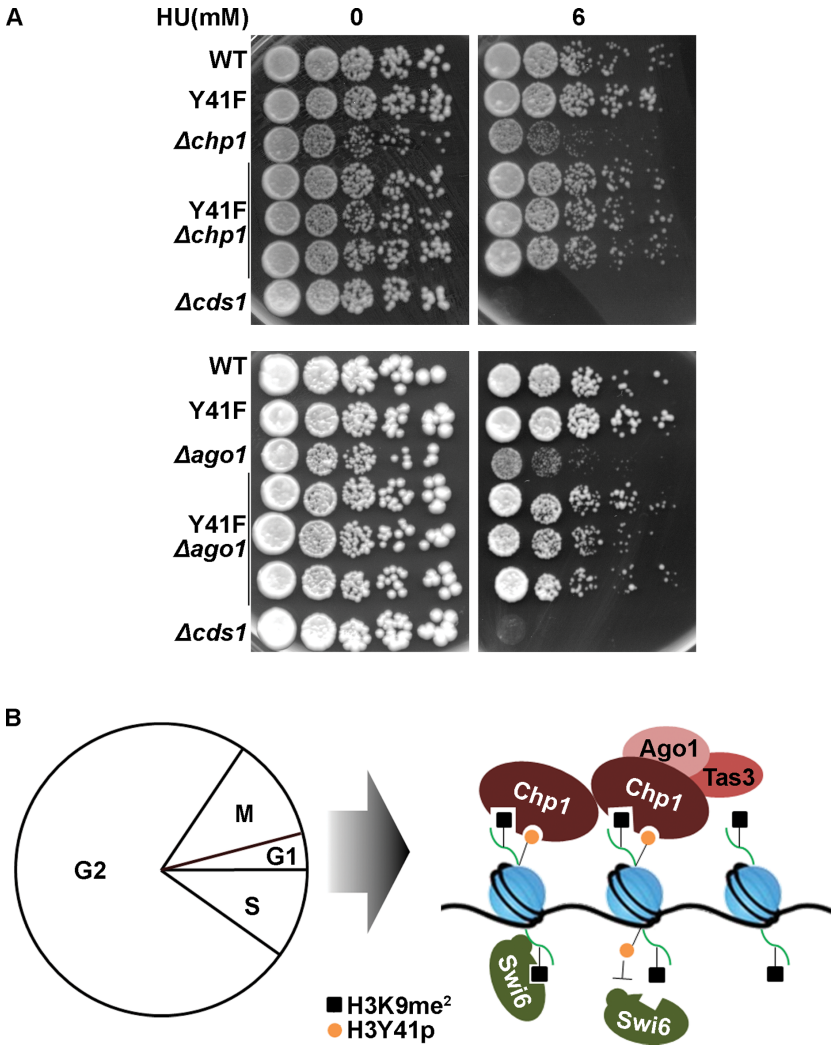

Figure 7. H3Y41p enhances the tolerance of RNAi mutants to the S-phase arresting agent hydroxyurea (HU). (**A**) Drug sensitivity test of 10-fold, serially diluted WT, Y41F, single RNAi mutants (top, *Δchp1*; bottom, *Δago1*) and double mutants with Y41F (top, Y41F*Δchp1*; bottom, Y41F*Δago1*) on 0 and 6 mM HU. *Δcds1* serves as a positive control on HU. (**B**) Model showing H3Y41p regulates the switch of heterochromatin binding proteins in M-early S phase.

sine residue to obstruct its phosphorylation (Y41F) would be expected to relieve the silencing effect, which is what we observed.

H3K9me2 is the major silencing hallmark in fission yeast heterochromatic regions; however, the H3K9me level did not change in conjunction with the restoration of silencing by Y41F, suggesting that H3Y41p may coordinate an alternative silencing pathway in parallel with H3K9me. The partial suppression of the silencing defect in a strain lacking the H3K9 histone methyltransferase Clr4 lends support to this potential regulation. Such complementation of H3K9me silencing defects may be mediated though the modulation of the chromatin scaffold; for example, by altering the acetylation status through regulating the activity and/or localization of the histone deacetylase. This is deduced from the inability of Y41F to suppress the heterochromatic silencing defects arising from the loss of SHREC histone deacetylase complex components. Through *in vitro* binding assays, we found that the interactions of Swi6 and Chp1 with H3K9me are more robust than their interactions with H3Y41. Given that H3Y41p could only partially cause delocalization of Swi6 when present with H3K9me, this points to the dominant role of H3K9me in heterochromatin formation. We believe that H3Y41p may have a contextual function in modulating silencing alongside H3K9me, presumably in addition to other anti-silencing mechanisms on the heterochromatic platform.

The preferential enrichment of H3Y41p on centromeric heterochromatin from M- until early S-phase of the cell cycle coincides with the dynamic remodeling of centromeric heterochromatin. Others have reported that, during this phase, Swi6 and H3K9me2 levels are reduced, and the RITS complex (Ago1 and Chp1) is recruited via its interaction with non-coding transcripts derived from pericentromeric heterochromatin. Rik1, as part of the CLRC complex, is also recruited at this stage (15,34). Pericentromeric heterochromatin replicates early, and contains replication origins that fire during the early part of S phase (59,60); and

this early-firing event is enforces by Swi6 (49). The timely phosphorylation of H3Y41 may reduce the affinity of Swi6 to methylated H3K9, which in turn leads to a reduction in residential time of Swi6 on centromeric heterochromatin, especially during S phase. It is possible that after initialising the replication origin, Swi6 is excluded from heterochromatin to permit heterochromatin decompaction, which is required for RNAPII accessibility, and this in turn leads to a spike in the transcription of heterochromatic DNA (33,34). The RNAPII-dependent transcription of centromeric repeat sequences preferentially occurs within a narrow window that overlaps with the recruitment of the RITS complex, and this is proposed to propagate the silenced chromatin onto the newly replicated DNA (51). Under these conditions, H3Y41 phosphorylation serves as a stabilization platform for the recruitment of Chp1 and, hence, RITS.

Switching between CD-containing proteins under the control of a single histone modification can offer an efficient and versatile coordination between DNA replication and the transcription of heterochromatic repeats. Proper coordination of these events is essential for cell viability, as the coexistence of DNA and RNA polymerases at the same location can cause them to crash into each other and cause genomic instability (51). As the cells pass into the G2 phase after replication, the switch is reversed, returning Swi6 levels via H3K4 acetylation (19). Based on these observations, we propose a model in which H3Y41p initiation of exclusion of Swi6 at the end of M-phase to facilitate the switch between Swi6 and Chp1 at pericentromeric heterochromatin at the entry of S phase. In so doing, H3Y41p works in concert with other mechanisms to localize heterochromatin proteins during the heterochromatic transcription window of S phase (Figure 7B). This capacity to alternately decompact and compact heterochromatin as required suggests that cells maintain efficient control over the S-phase window by switching between CD-containing proteins. This control safeguards epigenetic inheritance of the heterochromatic state while minimising the risk of genomic instability.

AVAILABILITY

The GEO accession code of RNA sequencing data is GSE102125.

SUPPLEMENTARY DATA

Supplementary Data are available at NAR online.

ACKNOWLEDGEMENTS

We would like to thank Yao Rui Ong and Kim Kiat Lim for technical assistance, Rebecca A. Jackson for editing this manuscript; Vivienne Jing Yi Tan and Cheryline Ruiling Tan for technical support during strain constructions; Mitsuhiro Yanagida, Matthew O'Connell and Yeast Genetic Resource Centre for strains, Hugh P. Cam and members of thesis advisory committee of B.R., Bor Luen Tang, Qiang Wu, Lih-Wen Deng and Yvonne Tay, for valuable comments.

FUNDING

Singapore Ministry of Education Tier I Grant [R-183-000-389-112]; Tier II Academic Research Fund [MOE2013-T2-1-112 awarded to E.S.C.]. Funding for open access charge: Singapore Ministry of Education Tier I Grant [R-183-000-389-112].
Conflict of interest statement. None declared.

REFERENCES

1. Jackson,R.A., Nguyen,M.L., Barrett,A.N., Tan,Y.Y., Choolani,M.A. and Chen,E.S. (2016) Synthetic combinations of missense polymorphic genetic changes underlying Down syndrome susceptibility. *Cell Mol. Life Sci.*, **73**, 4001–4017.
2. Ganmore,I., Smooha,G. and Izraeli,S. (2009) Constitutional aneuploidy and cancer predisposition. *Hum. Mol. Genet.*, **18**, R84–R93.
3. Luger,K., Dechassa,M.L. and Tremethick,D.J. (2012) New insights into nucleosome and chromatin structure: an ordered state or a disordered affair? *Nat. Rev. Mol. Cell Biol.*, **13**, 436–447.
4. Pueschel,R., Coraggio,F. and Meister,P. (2016) From single genes to entire genomes: the search for a function of nuclear organization. *Development*, **143**, 910–923.
5. Holoch,D. and Moazed,D. (2015) RNA-mediated epigenetic regulation of gene expression. *Nat. Rev. Genet.*, **16**, 71–84.
6. Rosenfeld,J.A., Wang,Z., Schones,D.E., Zhao,K., DeSalle,R. and Zhang,M.Q. (2009) Determination of enriched histone modifications in non-genic portions of the human genome. *BMC Genomics*, **10**, 143.
7. Cam,H.P., Sugiyama,T., Chen,E.S., Chen,X., FitzGerald,P.C. and Grewal,S.I. (2005) Comprehensive analysis of heterochromatin- and RNAi-mediated epigenetic control of the fission yeast genome. *Nat. Genet.*, **37**, 809–819.
8. Trojer,P. and Reinberg,D. (2007) Facultative heterochromatin: is there a distinctive molecular signature? *Mol. Cell*, **28**, 1–13.
9. Allshire,R.C. and Ekwall,K. (2015) Epigenetic Regulation of Chromatin States in *Schizosaccharomyces pombe*. *Cold Spring Harb. Perspect. Biol.*, **7**, a018770.
10. Allshire,R.C. and Karpen,G.H. (2008) Epigenetic regulation of centromeric chromatin: old dogs, new tricks? *Nat. Rev. Genet.*, **9**, 923–937.
11. Yanagida,M. (2005) Basic mechanism of eukaryotic chromosome segregation. *Philos. Trans. R Soc. Lond. B Biol. Sci.*, **360**, 609–621.
12. Zhang,K., Mosch,K., Fischle,W. and Grewal,S.I. (2008) Roles of the Clr4 methyltransferase complex in nucleation, spreading and maintenance of heterochromatin. *Nat. Struct. Mol. Biol.*, **15**, 381–388.
13. Verdel,A., Jia,S., Gerber,S., Sugiyama,T., Gygi,S., Grewal,S.I. and Moazed,D. (2004) RNAi-mediated targeting of heterochromatin by the RITS complex. *Science*, **303**, 672–676.
14. Sugiyama,T., Cam,H.P., Sugiyama,R., Noma,K., Zofall,M., Kobayashi,R. and Grewal,S.I. (2007) SHREC, an effector complex for heterochromatic transcriptional silencing. *Cell*, **128**, 491–504.
15. Motamedi,M.R., Verdel,A., Colmenares,S.U., Gerber,S.A., Gygi,S.P. and Moazed,D. (2004) Two RNAi complexes, RITS and RDRC, physically interact and localize to noncoding centromeric RNAs. *Cell*, **119**, 789–802.
16. Nakayama,J., Rice,J.C., Strahl,B.D., Allis,C.D. and Grewal,S.I. (2001) Role of histone H3 lysine 9 methylation in epigenetic control of heterochromatin assembly. *Science*, **292**, 110–113.
17. Rea,S., Eisenhaber,F., O'Carroll,D., Strahl,B.D., Sun,Z.W., Schmid,M., Opravil,S., Mechtler,K., Ponting,C.P., Allis,C.D. *et al.* (2000) Regulation of chromatin structure by site-specific histone H3 methyltransferases. *Nature*, **406**, 593–599.
18. Bannister,A.J., Zegerman,P., Partridge,J.F., Miska,E.A., Thomas,J.O., Allshire,R.C. and Kouzarides,T. (2001) Selective recognition of methylated lysine 9 on histone H3 by the HP1 chromo domain. *Nature*, **410**, 120–124.
19. Xhemalce,B. and Kouzarides,T. (2010) A chromodomain switch mediated by histone H3 Lys 4 acetylation regulates heterochromatin assembly. *Genes Dev.*, **24**, 647–652.
20. Bayne,E.H., White,S.A., Kagansky,A., Bijos,D.A., Sanchez-Pulido,L., Hoe,K.L., Kim,D.U., Park,H.O., Ponting,C.P., Rappsilber,J. *et al.* (2010) Stc1: a critical link between RNAi and

chromatin modification required for heterochromatin integrity. *Cell*, **140**, 666–677.
21. Noma,K., Sugiyama,T., Cam,H., Verdel,A., Zofall,M., Jia,S., Moazed,D. and Grewal,S.I. (2004) RITS acts in *cis* to promote RNA interference-mediated transcriptional and post-transcriptional silencing. *Nat. Genet.*, **36**, 1174–1180.
22. Debeauchamp,J.L., Moses,A., Noffsinger,V.J., Ulrich,D.L., Job,G., Kosinski,A.M. and Partridge,J.F. (2008) Chp1-Tas3 interaction is required to recruit RITS to fission yeast centromeres and for maintenance of centromeric heterochromatin. *Mol. Cell. Biol.*, **28**, 2154–2166.
23. Marasovic,M., Zocco,M. and Halic,M. (2013) Argonaute and Triman generate dicer-independent priRNAs and mature siRNAs to initiate heterochromatin formation. *Mol. Cell*, **52**, 173–183.
24. Moazed,D., Bühler,M., Buker,S.M., Colmenares,S.U., Gerace,E.L., Gerber,S.A., Hong,E.J., Motamedi,M.R., Verdel,A., Villén,J. *et al.* (2006) Studies on the mechanism of RNAi-dependent heterochromatin assembly. *Cold Spring Harb. Symp. Quant. Biol.*, **71**, 461–471.
25. Schalch,T., Job,G., Shanker,S., Partridge,J.F. and Joshua-Tor,L. (2011) The Chp1-Tas3 core is a multifunctional platform critical for gene silencing by RITS. *Nat. Struct. Mol. Biol.*, **18**, 1351–1357.
26. Sugiyama,T., Cam,H., Verdel,A., Moazed,D. and Grewal,S.I. (2005) RNA-dependent RNA polymerase is an essential component of a self-enforcing loop coupling heterochromatin assembly to siRNA production. *Proc. Natl. Acad. Sci. U.S.A.*, **102**, 152–157.
27. Colmenares,S.U., Buker,S.M., Buhler,M., Dlakić,M. and Moazed,D. (2007) Coupling of double-stranded RNA synthesis and siRNA generation in fission yeast RNAi. *Mol. Cell*, **27**, 449–461.
28. Smialowska,A., Djupedal,I., Wang,J., Kylsten,P., Swoboda,P. and Ekwall,K. (2014) RNAi mediates post-transcriptional repression of gene expression in fission yeast *Schizosaccharomyces pombe*. *Biochem. Biophys. Res. Commun.*, **444**, 254–259.
29. Grewal,S.I. and Jia,S. Heterochromatin revisited. *Nat. Rev. Genet.*, **8**, 35–46.
30. Steinhauf,D., Rodriguez,A., Vlachakis,D., Virgo,G., Maksimov,V., Kristell,C., Olsson,I., Linder,T., Kossida,S., Bongcam-Rudloff,E. *et al.* (2014) Silencing motifs in the Clr2 protein from fission yeast, *Schizosaccharomyces pombe*. *PLoS One*, **9**, e86948.
31. Motamedi,M.R., Hong,E.J., Li,X., Gerber,S., Denison,C., Gygi,S. and Moazed,D. (2008) HP1 proteins form distinct complexes and mediate heterochromatic gene silencing by nonoverlapping mechanisms. *Mol. Cell*, **32**, 778–790.
32. Cam,H.P., Chen,E.S. and Grewal,S.I. (2009) Transcriptional scaffolds for heterochromatin assembly. *Cell*, **136**, 610–614.
33. Chen,E.S., Zhang,K., Nicolas,E., Cam,H.P., Zofall,M. and Grewal,S.I. (2008) Cell cycle control of centromeric repeat transcription and heterochromatin assembly. *Nature*, **451**, 734–737.
34. Kloc,A., Zaratiegui,M., Nora,E. and Martienssen,R. (2008) RNA interference guides histone modification during the S phase of chromosomal replication. *Curr. Biol.*, **18**, 490–495.
35. Forsburg,S.L. and Rhind,N. (2006) Basic methods for fission yeast. *Yeast*, **23**, 173–183.
36. Nguyen,T.T., Chua,J.K., Seah,K.S., Koo,S.H., Yee,J.Y., Yang,E.G., Lim,K.K., Pang,S.Y., Yuen,A., Zhang,L. *et al.* (2016) Predicting hemotherapeutic drug combinations through gene network profiling. *Sci. Rep.*, **6**, 18658.
37. Tay,Z., Eng,R.J., Sajiki,K., Lim,K.K., Tang,M.Y., Yanagida,M. and Chen,E.S. (2013) Cellular robustness conferred by genetic crosstalk underlies resistance against chemotherapeutic drug doxorubicin in fission yeast. *PLoS One*, **8**, e55041.
38. Anders,S., Pyl,P.T. and Huber,W. (2015) HTseq|A Python framework to work with high-throughput sequencing data. *Bioinformatics*, **31**, 166–169.
39. Lim,K.K., Ong,T.Y., Tan,Y.R., Yang,E.G., Ren,B., Seah,K.S., Yang,Z., Tan,T.S., Dymock,B.W. and Chen,E.S. (2015) Mutation of histone H3 serine 86 disrupts GATA factor Ams2 expression and precise chromosome segregation in fission yeast. *Sci. Rep.*, **5**, 14064.
40. Dawson,M.A., Bannister,A.J., Göttgens,B., Foster,S.D., Bartke,T., Green,A.R. and Kouzarides,T. (2009) JAK2 phosphorylates histone H3Y41 and excludes HP1alpha from chromatin. *Nature*, **461**, 819–822.
41. Dawson,M.A., Foster,S.D., Bannister,A.J., Robson,S.C., Hannah,R., Wang,X., Xhemalce,B., Wood,A.D., Green,A.R., Göttgens,B. *et al.* (2012) Three distinct patterns of histone H3Y41 phosphorylation mark active genes. *Cell Rep.*, **2**, 470–477.
42. Brehove,M., Wang,T., North,J., Luo,Y., Dreher,S.J., Shimko,J.C., Ottesen,J.J., Luger,K. and Poirier,M.G. (2015) Histone core phosphorylation regulates DNA accessibility. *Biol. Chem.*, **290**, 22612–22621.
43. Hansen,K.R., Ibarra,P.T. and Thon,G. (2006) Evolutionary-conserved telomere-linked helicase genes of fission yeast are repressed by silencing factors, RNAi components and the telomere-binding protein Taz1. *Nucleic Acids Res.*, **34**, 78–88.
44. Zhou,Y. and Grummt,I. (2005) The PHD finger/bromodomain of NoRC interacts with acetylated histone H4K16 and is sufficient for rDNA silencing. *Curr. Biol.*, **15**, 1434–1438.
45. Johnson,A., Li,G., Sikorski,T.W., Buratowski,S., Woodcock,C.L. and Moazed,D. (2009) Reconstitution of heterochromatin-dependent transcriptional gene silencing. *Mol. Cell*, **35**, 769–781.
46. Sadaie,M., Kawaguchi,R., Ohtani,Y., Arisaka,F., Tanaka,K., Shirahige,K. and Nakayama,J. (2008) Balance between distinct HP1 family proteins controls heterochromatin assembly in fission yeast. *Mol. Cell. Biol.*, **28**, 6973–6988.
47. Soriano,I., Quintales,L. and Antequera,F. (2013) Clustered regulatory elements at nucleosome-depleted regions punctuate a constant nucleosomal landscape in *Schizosaccharomyces pombe*. *BMC Genomics*, **14**, 813.
48. Rustici,G., Mata,J., Kivinen,K., Lió,P., Penkett,C.J., Burns,G., Hayles,J., Brazma,A., Nurse,P. and Bähler,J. (2004) Periodic gene expression program of the fission yeast cell cycle. *Nat. Genet.*, **36**, 809–817.
49. Hayashi,M.T., Takahashi,T.S., Nakagawa,T., Nakayama,J. and Masukata,H. (2009) The heterochromatin protein Swi6/HP1 activates replication origins at the pericentromeric region and silent mating-type locus. *Nat. Cell Biol.*, **11**, 357–362.
50. Li,F., Martienssen,R. and Cande,W.Z. (2011) Coordination of DNA replication and histone modification by the Rik1-Dos2 complex. *Nature*, **475**, 244–248.
51. Zaratiegui,M., Castel,S.E., Irvine,D.V., Kloc,A., Ren,J., Li,F., de Castro,E., Marín,L., Chang,A.Y., Goto,D. *et al.* (2011) RNAi promotes heterochromatic silencing through replication-coupled release of RNA Pol II. *Nature*, **479**, 135–138.
52. Li,P.C., Petreaca,R.C., Jensen,A., Yuan,J.P., Green,M.D. and Forsburg,S.L. (2013) Replication fork stability is essential for the maintenance of centromere integrity in the absence of heterochromatin. *Cell Rep.*, **3**, 638–645.
53. Carmichael,J.B., Provost,P., Ekwall,K. and Hobman,T.C. (2004) Ago1 and Dcr1, two core components of the RNA interference pathway, functionally diverge from Rdp1 in regulating cell cycle events in *Schizosaccharomyces pombe*. *Mol. Biol. Cell*, **15**, 1425–1435.
54. Iida,T., Iida,N., Tsutsui,Y., Yamao,F. and Kobayashi,T. (2012) RNA interference regulates the cell cycle checkpoint through the RNA export factor, Ptr1, in fission yeast. *Biochem. Biophys. Res. Commun*, **427**, 143–147.
55. Yamada,T., Fischle,W., Sugiyama,T., Allis,C.D. and Grewal,S.I. (2005) The nucleation and maintenance of heterochromatin by a histone deacetylase in fission yeast. *Mol. Cell*, **20**, 173–185.
56. Luger,K., Mäder,A.W., Richmond,R.K., Sargent,D.F. and Richmond,T.J. (1997) Crystal structure of the nucleosome core particle at 2.8 A resolution. *Nature*, **389**, 251–260.
57. Rui,L., Emre,N.C., Kruhlak,M.J., Chung,H.J., Steidl,C., Slack,G., Wright,G.W., Lenz,G., Ngo,V.N., Shaffer,A.L. *et al.* (2010) Cooperative epigenetic modulation by cancer amplicon genes. *Cancer Cell*, **18**, 590–605.
58. Sadaie,M., Iida,T., Urano,T. and Nakayama,J. (2004) A chromodomain protein, Chp1, is required for the establishment of heterochromatin in fission yeast. *EMBO J.*, **23**, 3825–3835.
59. Hayashi,M., Katou,Y., Itoh,T., Tazumi,A., Yamada,Y., Takahashi,T., Nakagawa,T., Shirahige,K. and Masukata,H. (2007) Genome-wide localization of pre-RC sites and identification of replication origins in fission yeast. *EMBO J.*, **26**, 1327–1339.
60. Kim,S.M., Dubey,D.D. and Huberman,J.A. (2003) Early-replicating heterochromatin. *Genes Dev.*, **17**, 330–335.